Mechanism and Machine Theory 154 (2020) 104031

Contents lists available at ScienceDirect

Mechanism and Machine Theory

journal homepage: www.elsevier.com/locate/mechmachtheory

Research paper

Comparison of different optimal control formulations for generating dynamically consistent crutch walking simulations using a torque-driven model

Míriam Febrer-Nafría[a,*], Roger Pallarès-López[a], Benjamin J. Fregly[b], Josep M. Font-Llagunes[a]

[a] Department of Mechanical Engineering & Research Centre for Biomedical Engineering, Universitat Politècnica de Catalunya, Av. Diagonal, 647 08028 Barcelona, Spain
[b] Department of Mechanical Engineering, Rice University, 6100 Main St., 101 Mechanical Engineering Building, Houston, Texas 77005-1827 USA

ARTICLE INFO

Article history:
Received 7 May 2020
Revised 18 July 2020
Accepted 18 July 2020
Available online 28 July 2020

Keywords:
Biomechanics
Direct collocation optimal control
Optimization
Motion tracking
Crutch walking
Knee-ankle-foot orthosis

ABSTRACT

Walking impairment due to spinal cord injury can be improved using active orthoses, together with some type of external support such as crutches for balance. This study explores how optimal control problem formulation affects the ability to generate dynamically consistent crutch walking simulations with active orthosis assistance that closely reproduce experimental data. The investigation compares eight optimal tracking problem formulations using a torque-driven full-body skeletal model of a healthy subject walking with active knee-ankle-foot orthoses and forearm crutches. We have found that small adjustments to ground reactions are required to achieve convergence, tracking of joint instead of marker coordinates significantly improves convergence, and minimising joint jerks instead of joint accelerations has only a minor effect on the problem convergence. These results provide guidance for future work that seeks to develop predictive optimal control simulations that can identify orthosis control parameters that maximise improvement in walking function on an individual patient basis.

1. Introduction

Each year, between 250,000 and 500,000 people worldwide suffer a spinal cord injury (SCI) [1]. Walking impairment after SCI leads to a decreased quality of life, other serious health conditions (e.g., heart disease, high blood pressure), and substantial health care costs. Consequently, gait restoration is a high priority among people with SCI [2]. Restoration can be partially achieved using active orthoses or exoskeletons, together with some type of external support for balance (e.g., crutches or a walker) [3]. Because patients with SCI having the same clinical classification can exhibit high variability in their walking impairments, the control algorithms used in active orthoses need to be customised to maximise the walking ability of each patient. Such customisation is currently done through trial-and-error methods, making it difficult if not impossible to identify the best active control parameters for any particular patient.

* Corresponding author.
E-mail addresses: miriam.febrer@upc.edu (M. Febrer-Nafría), roger.pallares@estudiant.upc.edu (R. Pallarès-López), fregly@rice.edu (B.J. Fregly), josep.m.font@upc.edu (J.M. Font-Llagunes).

https://doi.org/10.1016/j.mechmachtheory.2020.104031
0094-114X/

Computational modelling provides a promising option for improving the customisation of assistive device controllers through movement simulation [4–7]. However, to date, few studies have used these methods to aid in the design of real wearable systems [8]. To this end, some challenges remain to be solved, such as finding the correct optimal control problem formulation for the generation of new assisted walking motions, or incorporating realistic models of technical assistive devices into a full-body musculoskeletal walking model [5]. Several studies exist that use optimal control methods to predict swing-through crutch gait using simple 2D human-crutch models [9,10], or four-point crutch gait using 3D human models without explicit modelling of arms and crutches [11]. Furthermore, recent studies have also used optimal control methods and simple 2D models to predict subject-exoskeleton combined motion when lifting a box using a lower back exoskeleton [8], or when performing a sit-to-stand transition using a lower limb exoskeleton [12].

In addition, at least two studies have simulated experimentally measured assisted walking motions using complex 3D full-body models, which integrate exoskeletons or orthoses and explicit models of arms and crutches [13,14]. In [13] the gait of five patients with SCI wearing an exoskeleton and using crutches was simulated using an inverse dynamics-based approach that used experimentally measured crutch-ground reaction forces and predicted foot-ground reaction forces. In [14] the gait of a subject with SCI wearing passive knee-ankle-foot orthoses (KAFOs) -with locked knee- and using crutches was simulated using a forward dynamics approach with joint controllers that tracked experimental trajectories. In this case, both crutch-ground and foot-ground reaction forces were predicted using compliant contact models. To the best of the authors' knowledge, no study in the literature has addressed how to formulate optimal control problems to generate crutch-assisted walking simulations using 3D full-body models including assistive lower limb devices and crutches.

Beyond assisted walking, predictive simulations of normal waking have been performed by solving optimal control problems (OCPs) using direct collocation [4,15–17] or direct multiple shooting [8,18–20]. Compared to shooting methods, direct collocation methods have the advantage of avoiding time-marching numerical integration of the equations of motion, eliminating the need to add stabilizing controllers when predicting walking motions. At the same time, these methods have the challenge of being sensitive to how the optimal control problem is formulated [21]. For human motion prediction, direct collocation problems have worked best when model dynamics is formulated implicitly rather than explicitly [17,22]. Moreover, as suggested by two studies [4,17], direct collocation optimal control could also provide a valuable approach for customising the active control of lower extremity orthoses or exoskeletons to the needs of individual patients with neurological impairments. When these predictions are made using 3D complex models, a common approach is to solve an optimal tracking problem first that finds a dynamically consistent walking motion (i.e., with all residual loads acting on the pelvis being below a small tolerance) that is as consistent as possible with all available experimental data, and then to use the tracking results as the initial guess for predicting a novel walking motion [11,17]. However, lately some authors have succeeded to perform predictive gait simulations using non data-driven initial guesses [23,24].

This study explores how direct collocation optimal control problem formulation affects convergence of optimal tracking problems for crutch-assisted walking of a subject wearing active KAFOs. Identifying the most efficient and robust optimal tracking problem formulation for crutch-orthosis-assisted walking is a logical first step toward solving optimal control problems that generate new crutch-orthosis-assisted walking motions, since their mathematical formulation will have a very similar structure. The study builds on recent work aimed at the development of an innovative, affordable, lightweight, and customised active KAFO [25] to assist over-ground walking of patients with SCI. Specifically, target patients retain some hip muscle function, so that they can initiate swing using these muscles, but lack control of knee and ankle muscles. A systematic review of active KAFOs for gait rehabilitation can be found in [26]. To identify the most efficient and robust optimal tracking problem formulation, we investigated eight options involving different methods for achieving dynamic consistency and reproducing experimentally measured motion data. All eight optimal tracking problems were solved using GPOPS-II direct collocation optimal control software applied to a torque-driven full-body skeletal model with forearm crutches implemented in OpenSim musculoskeletal modelling software [27,28]. To provide experimental walking data for performing the investigation, we collected marker motion and ground reaction data from a single healthy subject who wore bilateral active KAFOs while walking with forearm crutches. The results provide insight into which aspects of the optimal tracking problem formulation affect achievement of convergence and which aspects affect speed of convergence.

2. Materials and methods

2.1. Experimental data collection

To provide an initial dataset for identification of the best optimal control problem formulation, we collected experimental orthosis-assisted crutch walking data from a healthy female subject (age 27 yrs., mass 52 kg, height 1.62 m) at the UPC Motion Analysis Laboratory in the Department of Mechanical Engineering of the Barcelona School of Industrial Engineering (ETSEIB). The study was approved by the Research Committee of UPC, which handles ethical issues involved in research projects, and the subject gave written informed consent for experimental data collection and subsequent data use for modelling purposes. The subject wore a pair of identical active KAFOs and used forearm crutches (Fig. 1, centre). The followed crutch walking pattern was a four-point pattern, being the swing phases sequence within the walking cycle: left leg, left crutch, right leg, right crutch. The powered KAFO used in our study (Fig. 1, left) has an actuation system (electrical motor plus Harmonic Drive gearbox) that locks the knee joint during stance phase, and flexes and extends the knee joint during swing phase by following a predefined knee angle trajectory. The ankle is passively actuated by a compliant joint that

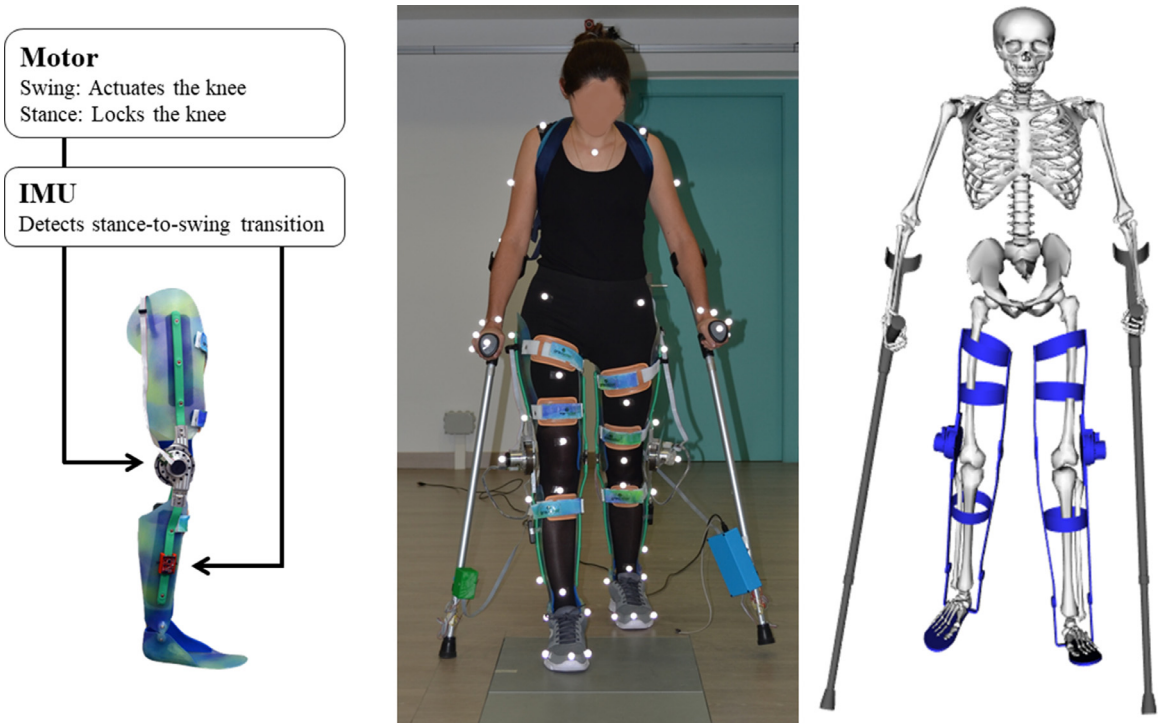

Fig. 1. The active KAFO (left), the healthy subject during the experimental data collection (centre), and the computational multibody model developed in OpenSim (right).

avoids drop-foot gait. The stance-to-swing transition event is automatically identified by means of two inertial measurement units (IMUs) attached to the shank supports of both orthoses. Moreover, the user wears a backpack that contains an embedded computer board, the motor drivers, and the power supply unit. The reader is referred to [25] for more detailed information about this device. For active orthosis assistance, the motor control system limited maximum knee flexion during swing phase to 40°. Data were collected from a healthy subject, instead of a patient with SCI, since data collection with a healthy subject is less complicated (e.g., it is easier for a healthy subject to step on each force plate with one foot and no crutch contact) and the computational issues being explored in this study can be explored equally well regardless of the status of the subject. Although hip and ankle joints were actuated by the healthy subject's muscles; the orthosis is intended for SCI patients who preserve some motor function at the hip, but cannot control ankle muscles. Moreover, the orthosis kinematic performance is the same for a healthy subject or a patient with SCI, as the knee controller follows a predefined flexion-extension angle and the IMUs detect the stance-to-swing event the same way in both cases.

Experimental walking data consisted of marker trajectories, foot-ground reaction forces and moments, and crutch-ground reaction forces. Surface marker motion was recorded at 100 Hz by tracking 43 passive reflective markers using 16 optical infrared cameras (OptiTrack V100:R2, NaturalPoint Inc., Corvallis, OR, USA). Ground reaction forces and moments were measured at the same sampling frequency by two force plates (AccuGait, AMTI, Watertown, MA, USA) located in the floor at the centre of the capture workspace. A pair of crutches were instrumented with tri-axial load cells at the tips to measure crutch-ground contact force components at 10 Hz following the approach used in [29]. Kinematic, force plate, and crutch load cell data were synchronized. Data were exported to MATLAB, where filtering was performed. Foot-ground reaction force and moment components were filtered using a 3rd-order zero phase lag Butterworth filter with cut-off frequency of 6 Hz. Crutch-ground reaction force components were resampled to 100 Hz, filtered using the same filter, and transformed to the global reference frame.

2.2. Torque-driven walking model

A three-dimensional torque-driven full-body walking model of the healthy subject using the active orthoses and crutches was created starting from a published full-body OpenSim model [30]. The model was composed of 12 segments: pelvis, torso (including head), two upper arms, two forearms (including hands), two thighs, two shanks and two feet. Two model degrees of freedom (DOF) were modified to adapt the previous OpenSim model to this study, i.e., the right and left forearm pronation/supination angles were locked at 90°. Therefore, the modified multibody model possessed 27 DOFs: 6 DOFs between the ground and pelvis, 3 for the lumbo-sacral joint, 3 for each shoulder, 1 for each elbow, 3 for each hip, 1 for each knee, and 1 for each ankle (Fig. 1, right). The associated 27 model or joint coordinates $\boldsymbol{q}$ were: 3 pelvis translations

Table 1
Top of the table: Initial residual values, obtained from ID using experimental data: maximum, minimum and RMS of each force and moment (AP: anterior-posterior, V: vertical, ML: mediolateral). Bottom of the table: tolerances for half and full residual reduction (upper and lower bounds, corresponding to the positive and negative values for each tolerance). Half of RMS value for each residual force and moment corresponds to the half reduction tolerance values.

		F_{AP} (N)	F_V (N)	F_{ML} (N)	M_{AP} (Nm)	M_V (Nm)	M_{ML} (Nm)
Initial values	**MAX**	22.99	38.77	22.65	10.80	7.49	22.59
	MIN	-11.04	-63.70	-26.31	-17.84	-5.56	-21.72
	RMS	9.28	22.81	9.81	6.56	2.57	9.73
Half reduction tolerances		4.64	11.40	4.90	3.28	1.28	4.86
Full reduction tolerances		0.1	0.1	0.1	0.01	0.01	0.01

(anterior-posterior, vertical, mediolateral), 3 pelvis rotations (tilt, list, rotation), 3 lumbar rotations (extension, bending, rotation), 3 shoulder rotations (flexion, adduction, rotation) for left and right sides, 1 elbow rotation (flexion) for left and right sides, 3 hip rotations (flexion, adduction, rotation) for left and right sides, 1 knee rotation (flexion) for left and right sides, and 1 ankle rotation (flexion) for left and right sides. Finally, the model was scaled to the subject using marker data from a static trial and the OpenSim Scale Model Tool. In this step, we considered the backpack mass as attached to the torso segment.

The orthoses were modelled as independent bodies consisting of three segments (corresponding to thigh, shank and foot) with dimensions and inertial properties taken from CAD models of the prototype. Each orthosis segment was attached to the corresponding lower limb segment using a weld joint (i.e., no relative motion was permitted between bodies). No joints were defined between the orthosis segments, i.e., knee and ankle orthosis joints were considered perfectly aligned to the subject's joints. The two crutches were added to the model initially with 6 DOF relative motion with respect to each corresponding forearm. To determine constant values for these generalized coordinates, we performed an OpenSim Inverse Kinematics (IK) analysis [27], calculated the mean value for each translational and rotational coordinate, and finally added a weld joint consistent with these mean values to replace each 6 DOF joint.

The OpenSim IK and Inverse Dynamics (ID) Tools were used to calculate joint motions for the full-body model and the initial residual forces and moments applied to the pelvis segment [27,30]. In the IK problem, all weights for tracking marker coordinates were set to 1. Since only two force plates were available in the lab, we did not have foot-ground reactions (forces and moments) for a complete gait cycle. Therefore, we simulated a partial gait cycle that began at left toe off, which occurred at 18% of the subject's full gait cycle, and finished with right crutch strike, which corresponds to the 100% of the gait cycle. We translated the foot-ground reactions from the centre of the force plates to the origin of each calcaneus to facilitate performing ID with the OpenSim C++ Application Programming Interface (API). Using the joint motions found from IK, we performed ID to determine the initial residual loads (i.e., forces and moments) relative to the pelvis origin (Table 1).

2.3. Optimal control problem formulations

To obtain dynamically consistent walking motions with our OpenSim model, we used direct collocation optimal control to formulate optimal tracking problems that constrained the residual forces and moments acting on the pelvis below a small tolerance [17,31]. An optimal control problem can be stated in the following general form: Determine the state and control that minimise a cost functional subject to specified constraints [32]. In human motion prediction, design variables of an optimal control problem can be related to motion (e.g., generalised coordinates, velocities, accelerations), forces (e.g., joint torques, muscle activations), or parameters of the predicted motion (e.g., mean speed, duration of each phase, step length). Control variables do not need to be physical controls and are usually time varying quantities whose derivatives are not needed in the problem solution process.

As mentioned in [22], implicit skeletal dynamics (e.g., $F\text{-}m\cdot a = 0$) works better than explicit skeletal dynamics (e.g., $a = F/m$) when solving direct collocation optimal control problems involving human movement. The OCP solver used in this work, GPOPS-II [33], does not handle implicit dynamics and requires the use of explicit dynamics for dynamic constraints. We addressed this limitation by putting an implicit form of skeletal dynamics in the path constraints, making joint acceleration or jerk additional controls, and using kinematic derivative relationships (e.g., joint jerk equals the first time derivative of joint acceleration, joint acceleration equals the first time derivative of joint velocity, etc.) for the required explicit dynamics. To make the controls unique, we added a joint acceleration or jerk regularisation term to the cost function. Although this term is not related to any physiological criterion, it has been employed in previous studies to improve convergence by making the solution unique [17,34,35]. However, it is still unknown if one type of control (joint acceleration or joint jerk) is advantageous over the other.

To identify the most efficient and robust approach for generating dynamically consistent orthosis-assisted crutch walking simulations, we explored eight different optimal control problem formulations (Table 2). All problems involved combinations of tracking marker coordinates versus tracking joint coordinates, tracking ground reactions (foot-ground reaction forces and moments and crutch-ground reaction forces) versus not imposing them, and minimising joint acceleration versus joint jerk. Optimal control problem formulations were labelled, A, B, C, and D, with two cases being explored for each formulation.

Table 2
Description of the eight different formulations that have been compared in this study. Variables correspond to markers coordinates ($\boldsymbol{m}$), joint coordinates ($\boldsymbol{q}$), joint velocities ($\dot{\boldsymbol{q}}$), joint accelerations ($\ddot{\boldsymbol{q}}$), joint jerks ($\dddot{\boldsymbol{q}}$) and ground reactions (foot-ground forces and moments and crutch-ground forces) ($\boldsymbol{GR}$).

Formulation	Track	Minimise	States	Controls
A1	$\boldsymbol{m}$	$\ddot{\boldsymbol{q}}$	$\boldsymbol{q}, \dot{\boldsymbol{q}}$	$\ddot{\boldsymbol{q}}$
A2		$\dddot{\boldsymbol{q}}$	$\boldsymbol{q}, \dot{\boldsymbol{q}}, \ddot{\boldsymbol{q}}$	$\dddot{\boldsymbol{q}}$
B1	$\boldsymbol{q}$	$\ddot{\boldsymbol{q}}$	$\boldsymbol{q}, \dot{\boldsymbol{q}}$	$\ddot{\boldsymbol{q}}$
B2		$\dddot{\boldsymbol{q}}$	$\boldsymbol{q}, \dot{\boldsymbol{q}}, \ddot{\boldsymbol{q}}$	$\dddot{\boldsymbol{q}}$
C1	$\boldsymbol{m} + \boldsymbol{GR}$	$\ddot{\boldsymbol{q}}$	$\boldsymbol{q}, \dot{\boldsymbol{q}}$	$\ddot{\boldsymbol{q}}, \boldsymbol{GR}$
C2		$\dddot{\boldsymbol{q}}$	$\boldsymbol{q}, \dot{\boldsymbol{q}}, \ddot{\boldsymbol{q}}$	$\dddot{\boldsymbol{q}}, \boldsymbol{GR}$
D1	$\boldsymbol{q} + \boldsymbol{GR}$	$\ddot{\boldsymbol{q}}$	$\boldsymbol{q}, \dot{\boldsymbol{q}}$	$\ddot{\boldsymbol{q}}, \boldsymbol{GR}$
D2		$\dddot{\boldsymbol{q}}$	$\boldsymbol{q}, \dot{\boldsymbol{q}}, \ddot{\boldsymbol{q}}$	$\dddot{\boldsymbol{q}}, \boldsymbol{GR}$

Formulations A tracked marker coordinates, formulations B tracked joint coordinates, formulations C tracked marker coordinates and ground reactions, and formulations D tracked joint coordinates and ground reactions. In all formulations, joint coordinates and velocities were problem states. In formulations A and B, the experimentally measured ground reactions were applied directly to the model. In formulations C and D, additional controls representing the ground reactions were added to the design variables. These controls tracked the experimental ground reactions and were applied to the model in place of those experimental values. Though this approach created a more complicated optimal control problem, it allowed for slight adjustments in the ground reactions to account for both measurement and modelling errors if needed. For each of these four problem formulations, we studied two cases: one case used joint accelerations as controls and minimised them in the cost function (case 1), while the other case used joint jerks as controls, minimised them in the cost function, and added joint accelerations as an additional state (case 2). As an example, the cost functional corresponding to formulation A1 is:

$$J = \int_{t_0}^{t_f} (\boldsymbol{m} - \boldsymbol{m}_{\text{exp}})^T (\boldsymbol{m} - \boldsymbol{m}_{\text{exp}}) + \ddot{\boldsymbol{q}}^T \ddot{\boldsymbol{q}}\, dt \tag{1}$$

where $\boldsymbol{m}$ stands for the vector of marker coordinates, $\boldsymbol{m}_{exp}$ the vector of experimental marker coordinates, and $\ddot{\boldsymbol{q}}$ the vector of joint accelerations (second time derivative of $\boldsymbol{q}$).

In all eight formulations, dynamic constraints were simple relations among design variables, since some kinematic variables were the derivatives of the others (e.g., the first time derivative of joint velocity is joint acceleration). For instance, for formulation A1:

$$\left[\frac{d\boldsymbol{q}}{dt}, \frac{d\dot{\boldsymbol{q}}}{dt}\right]^T = \left[\dot{\boldsymbol{q}}, \ddot{\boldsymbol{q}}\right]^T \tag{2}$$

An ID Analysis was performed at each iteration using the OpenSim C++ API (version 3.3) (Fig. 2). The system kinematic state was used to calculate the net forces and torques applied to each DOF. Path constraints limited the residual loads acting on the pelvis $\boldsymbol{R}_{pelvis}$ to be within a specific tolerance $\boldsymbol{\varepsilon}$ [17,31]:

$$-\boldsymbol{\varepsilon} \leq \boldsymbol{R}_{pelvis}\left(\boldsymbol{q}, \dot{\boldsymbol{q}}, \ddot{\boldsymbol{q}}\right) \leq \boldsymbol{\varepsilon} \tag{3}$$

Two different sets of tolerances were considered: half residual reduction and full residual reduction (Table 1). The first one was defined as achieving half of the root mean square (RMS) of the initial residual loads, which resulted in tolerances less than 5 N or 5 Nm, with the exception of the normal force that was 11.40 N. The second set of tolerances were 0.1 N for forces and 0.01 Nm for moments. Although a solution with residuals reduced to the first set of tolerances could be considered good enough [36], we wanted to investigate the convergence and solution achieved when residuals were reduced to the second set of tolerances. The solutions were obtained independently for both sets of tolerances. Five different initial guesses were used, two based on the experimental data, one using constant values [21], and two non data-driven (random or quasi-random) [23,24]: (1) Experimental data (239 points), (2) Experimental data taking every 10th point (24 points), (3) Experimental mean values (10 points), (4) Sinusoidal signals of random amplitude and random phase (10 points), (5) Sinusoidal signals of random amplitude and random phase (100 points). A maximum value for amplitude was given to the random signals based on the maximum values of the experimental data (e.g., 20° for all joint angles, 5 rad/s for angular velocities, 500 N for normal forces). For each variable, a different signal was computed for cases (4) and (5). The same initial guesses (4) and (5) were used for all different formulations.

All optimal control problems were solved using the software GPOPS-II [33], which utilises a direct collocation method. GPOPS-II transcribes optimal control problems into corresponding non-linear programming problems. Our solution process used the built-in interior point optimisation algorithm (IPOPT) [37], employing the linear solver 'mumps' with a maximum

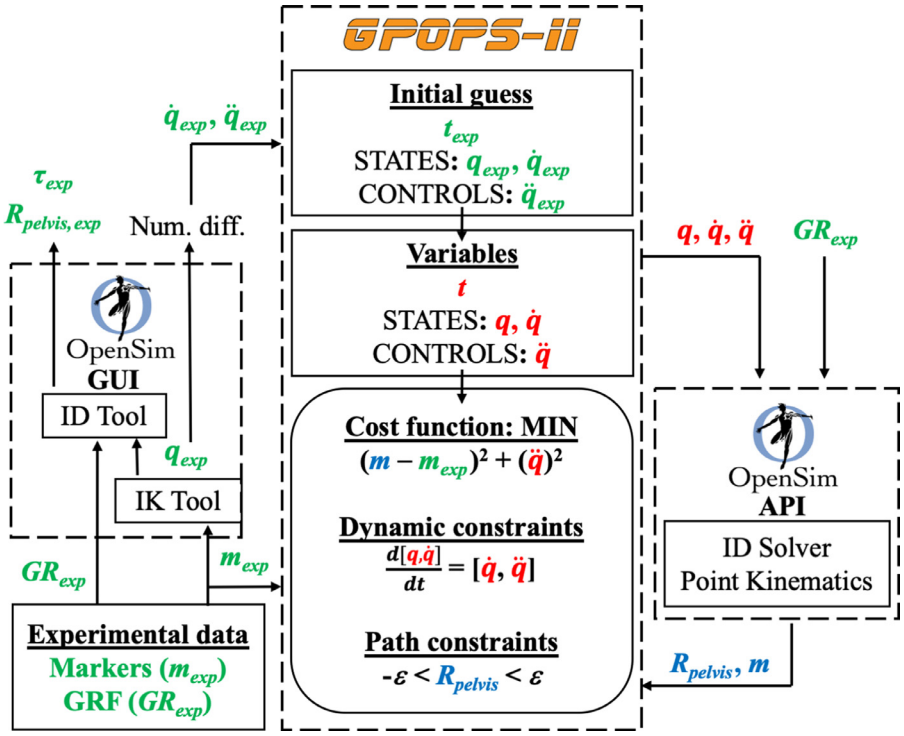

Fig. 2. Scheme of the prediction framework for Formulation A1. Previous to the OCP solution, IK and ID were performed in the OpenSim GUI. At each iteration, ID is solved and the model markers positions are obtained using OpenSim API. The colour legend is the following: green indicates variables that are measured experimentally or calculated directly from experimental measurements, red indicates variables of the OCP, and blue indicates magnitudes that are computed at each iteration. Variables correspond to marker coordinates ($\boldsymbol{m}$), joint coordinates ($\boldsymbol{q}$), joint velocities ($\dot{\boldsymbol{q}}$), joint accelerations ($\ddot{\boldsymbol{q}}$), ground reactions (foot-ground forces and moments and crutch-ground forces) ($\boldsymbol{GR}$), joint torques ($\boldsymbol{\tau}$) and residuals ($\boldsymbol{R}_{pelvis}$). Subscript *exp* indicates an experimental value: experimental marker coordinates and ground reactions were measured directly, while experimental joint coordinates, torques and residuals were obtained from IK and ID performed in OpenSim, respectively. For more information about IK and ID algorithms in OpenSim, the reader is referred to [27,30]. (For interpretation of the references to colour in this figure legend, the reader is referred to the web version of this article.)

of 10,000 iterations on an initial grid of 10 mesh intervals and 4 collocation points per interval. The IPOPT convergence tolerance was set to 10^{-4}, and the solution mesh tolerance was set to 10^{-3}. Design variables and experimental quantities were scaled such that their maximum initial values were around one. The scaling factors were applied to basic magnitudes: mass (0.25), length (2), angle (1), and time (10). And from them, all the other magnitudes were scaled consistently (e.g., linear velocity scaling factor = length scaling factor / time scaling factor). In this way, errors in the cost function were comparable, and all terms in the cost function where equally weighted as shown in Eq. (1). All optimisations were performed using a Dell Precision Tower 5810 (Intel(R) Xeon(R) CPU E5-1620 v3 @ 3.50GHz, 16.00 GB RAM).

To compare the different optimal control formulations, we calculated several metrics for each level of pelvis residual reduction (half and full). These metrics included the number of iterations and computation time needed to reach each optimal solution and the RMS error (RMSE) between predicted values (marker coordinates, joint coordinates, joint torques and ground reaction forces and moments) and corresponding experimental values. Experimental marker coordinates and ground reactions were measured directly, while experimental joint coordinates and experimental joint torques were obtained from OpenSim IK and ID analyses performed using the experimental marker coordinates and ground reactions.

3. Results

Convergence was better overall for half residual reduction, and full residual reduction converged only when both motion and ground reactions were adjusted (Table 3). Thus, ground reaction adjustments were required if a dynamically consistent motion with residual values close to zero was to be found. For the optimisations that converged, there was no remarkable difference in the reduction of residuals among formulations, as they were reduced to the imposed tolerance in all cases. The number of iterations and computation time varied for each different initial guess, but the obtained solution for each guess was the same for each formulation. For formulations that tracked marker coordinates, the number of iterations (and consequently, computation time) was higher for full residual reduction compared to half residual reduction; whereas for formulations that tracked joint coordinates, the number of iterations and computation time were higher for half residual reduction compared to full residual reduction (Table 3, right columns). There was practically no difference in terms of mean RMSE for marker coordinates and angular joint coordinates for half residual reduction compared to full residual reduction.

Table 3
Mean and standard deviation of number of iterations and computation time, mean and standard deviation of RMSE of marker and joint coordinates, joint torques, GRFs (foot- and crutch-ground) and GRMs (foot-ground) for each formulation and residual reduction tolerance. Mean and standard deviation of number of iterations and computation time have been computed for all five results (one per each initial guess) for each formulation. Mean and standard deviation of RMSEs have been computed for results using the initial guess based on experimental data with all points (first initial guess). Results are shown per two different tolerances of residual reduction: half and full. Mean and standard deviation of RMSE of each magnitude are shown in black when they are tracked in the formulation, and in grey when they are not. With '-', we indicate that those variables are not included in the formulation, and with 'x', that the problem has not converged. "Conv." stands for convergence, "Marker" and "Joint" stand for marker and joint coordinates, respectively.

			Without ground-reaction adjustment				With ground-reaction adjustment			
			Track marker coordinates		Track joint coordinates		Track marker coordinates		Track joint coordinates	
			Min acc. A1	Min jerk A2	Min acc. B1	Min jerk B2	Min acc. C1	Min jerk C2	Min acc. D1	Min jerk D2
Half residual reduction	**Conv.**	Iterations	296.80 ± 79.90	321.60 ± 83.93	25.80 ± 4.60	25.60 ± 4.39	360.20 ± 49.18	411.80 ± 65.19	87.60 ± 8.17	102.40 ± 6.07
		Time [min]	53.42 ± 20.90	55.46 ± 31.45	1.24 ± 0.16	1.61 ± 0.21	59.47 ± 9.54	88.87 ± 21.73	4.61 ± 0.40	6.77 ± 0.45
	RMSE	Marker [cm]	1.52 ± 0.70	1.46 ± 0.69	2.21 ± 1.07	2.25 ± 1.09	1.12 ± 0.65	1.06 ± 0.65	1.20 ± 0.73	1.17 ± 0.73
		Joint [cm]	0.93 ± 0.23	0.88 ± 0.33	0.83 ± 0.39	0.82 ± 0.38	0.40 ± 0.06	0.31 ± 0.08	0.36 ± 0.21	0.34 ± 0.22
		Joint [°]	4.36 ± 2.42	3.99 ± 2.29	1.32 ± 0.83	1.32 ± 0.84	3.02 ± 1.94	2.26 ± 1.48	0.83 ± 0.44	0.74 ± 0.43
		Torques [Nm]	82.91 ± 114.79	83.11 ± 114.52	82.41 ± 112.56	82.53 ± 112.56	1.90 ± 1.37	1.73 ± 1.27	1.46 ± 1.23	1.47 ± 1.19
		GRFs [N]	-	-	-	-	7.13 ± 13.97	7.10 ± 13.99	6.65 ± 14.20	6.66 ± 14.19
		GRMs [Nm]	-	-	-	-	0.17 ± 0.08	0.19 ± 0.07	0.06 ± 0.04	0.07 ± 0.05
Full residual reduction	**Conv.**	Iterations	x	x	x	x	531.20 ± 388.24	1400.80 ± 636.06	63.40 ± 12.46	68.20 ± 12.38
		Time [min]	x	x	x	x	101.61 ± 99.83	326.33 ± 109.16	3.49 ± 0.69	4.73 ± 0.85
	RMSE	Marker [cm]	x	x	x	x	1.17 ± 0.64	1.12 ± 0.63	1.33 ± 0.71	1.31 ± 0.71
		Joint [cm]	x	x	x	x	0.52 ± 0.05	0.45 ± 0.01	0.54 ± 0.19	0.54 ± 0.20
		Joint [°]	x	x	x	x	3.04 ± 1.99	2.31 ± 1.49	0.85 ± 0.43	0.77 ± 0.42
		Torques [Nm]	x	x	x	x	2.55 ± 1.56	2.36 ± 1.42	2.10 ± 1.52	2.11 ± 1.50
		GRFs [N]	-	-	-	-	8.06 ± 13.73	8.03 ± 13.74	7.66 ± 13.91	7.67 ± 13.90
		GRMs [Nm]	-	-	-	-	0.46 ± 0.09	0.45 ± 0.10	0.18 ± 0.13	0.20 ± 0.13

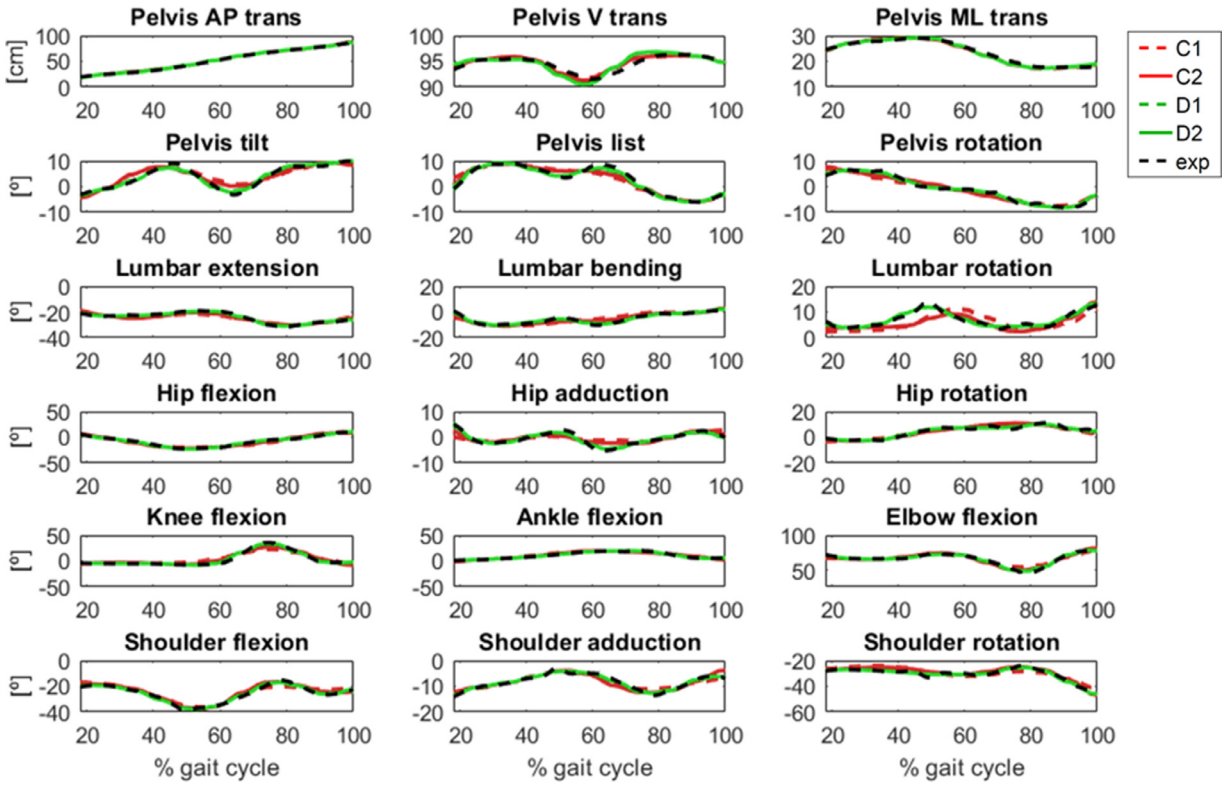

Fig. 3. Coordinates obtained in formulations C and D for the full residual reduction compared to experimental values. Results for each one of the five initial guesses are plotted for each formulation. Note that all five initial guesses converge to the same solution, as no difference is appreciated between curves from the same formulation. Results are shown for pelvis, torso, right leg and right arm. Symmetry is not imposed, but results for left and right side are similar. In the figure AP, V and ML stand for anterior-posterior, vertical and mediolateral, respectively.

The mean RMSE of linear joint coordinates was larger in the case of full residual reduction (0.54 cm, 0.54 cm) compared to half residual reduction (0.36 cm, 0.34 cm) for formulations D. The mean RMSE for ground reaction forces (GRFs) and ground reaction moments (GRMs) for half residual reduction were between 6.65 and 7.13 N and between 0.06 and 0.19 Nm, respectively. For full residual reduction, these values were up to 1.01 N and 0.29 Nm higher than those obtained for half residual reduction using the same formulation. Regarding joint torques, mean RMSEs were lower when ground reactions were adjusted (around 83 Nm for formulations A and B, and less than 2 Nm for formulations C and D, for the case of half residual reduction), and results were similar when marker or joint coordinates were tracked (Fig. 5).

More iterations and computation time were needed when tracking marker coordinates rather than joint coordinates. For full residual reduction, tracking marker coordinates required 531 and 1400 iterations, resulting in 102 min (1 h 42 min) and 326 min (5 h 26 min), whereas tracking joint coordinates required 63 and 68 iterations, resulting in 3.49 min and 4.73 min (Table 3, right bottom). Mean RMSEs for marker and joint coordinates were in general lower when they were tracked compared to when they were not tracked. Mean RMSEs for marker coordinates were 1.17 cm and 1.12 cm when they were tracked (formulations C), and 1.33 cm and 1.31 cm when they were not (formulations D). Mean RMSEs for angular joint coordinates were 0.85° and 0.77° when they were tracked (formulations D), and 3.04° and 2.31° when they were not (formulations C) (Fig. 3). Ground reaction force and moment errors were slightly larger when tracking marker coordinates (up to 8.06 N and 0.46 Nm) compared to tracking joint coordinates (up to 7.67 N and 0.20 Nm) (Fig. 4).

There were practically no differences in motion and forces between minimising joint acceleration or joint jerk for full residual reduction (Figs. 3 and 4). In terms of number of iterations (and consequently, computation time), for formulations C, fewer iterations (around 2.6x less) were needed when minimising joint acceleration rather than joint jerk. In contrast, for formulations D, a similar number of iterations (63 and 68) were needed when minimising joint acceleration or joint jerk, respectively. When comparing tracking errors, differences between mean RMSE within each formulation (C and D) for minimising joint acceleration or joint jerk were less than 0.05 cm for marker coordinates, 0.07 cm for linear joint coordinates, 0.73° for angular joint coordinates, 0.19 Nm for joint torques, 0.03 N for ground reaction forces, and 0.02 Nm for ground reaction moments.

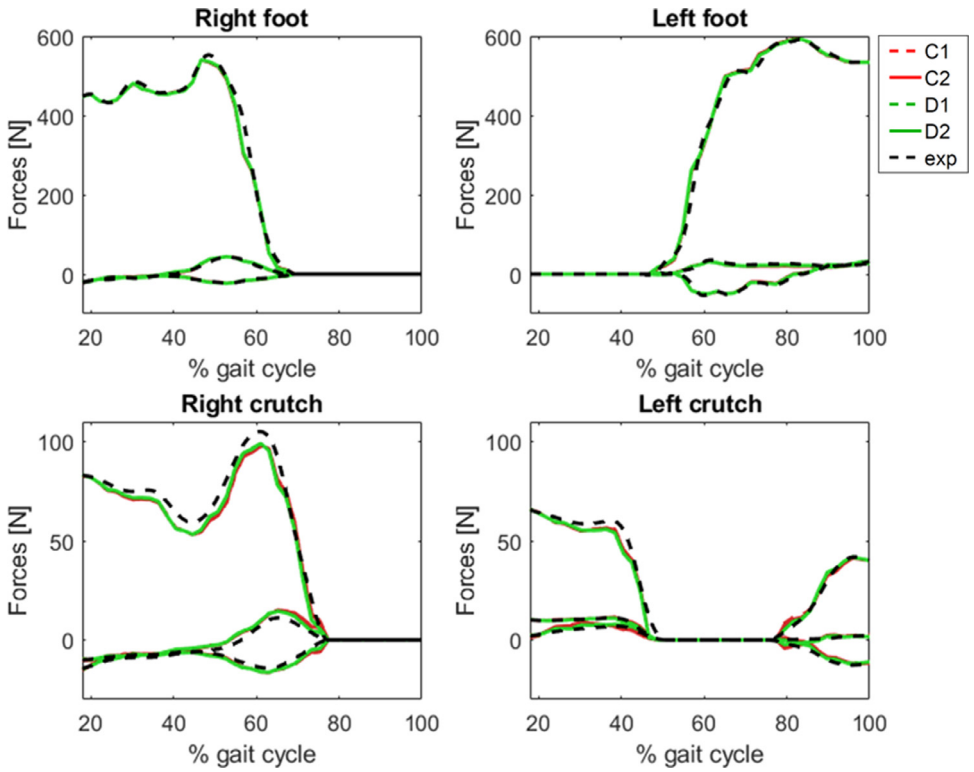

Fig. 4. Foot- and crutch-ground reaction forces obtained in formulations C and D for full residual reduction tolerances compared to experimental values. Results for each one of the five initial guesses are plotted for each formulation. Note that all five initial guesses converge to the same solution, as no difference is appreciated between curves from the same formulation. Only forces (in the global reference frame) have been plotted. The larger component in each case is in the vertical direction.

4. Discussion

This study compared eight optimal control problem formulations that tracked experimental walking data from a healthy subject using crutches and active orthoses. The goal was to identify the best optimal control problem formulation that generated a dynamically consistent assisted-walking motion as a first step toward using predictive optimal control for virtually testing different active knee control strategies. Optimal control was used to track an experimental orthosis-assisted crutch walking motion to obtain a dynamically consistent movement. For the present study, the controller used by the active orthosis was predefined in the experimental device. Five different initial guesses were used to test the robustness of the formulation, and all them converged to the same solution. We found that optimal control problems converged more rapidly when tracking joint coordinates rather than marker coordinates. We also found that convergence was improved when ground reactions were included as additional controls that tracked experimental measurements. Finally, we found that minimisation of joint jerk generally resulted in slightly better tracking of marker coordinates, joint coordinates, joint torques and ground reactions than did minimisation of joint acceleration and with comparable computation time. Overall, the formulations that converged with lowest mean RMSE, for both half and full residual reduction, were the ones that tracked joint coordinates and ground reactions, both minimising joint acceleration and jerk (formulations D1 and D2, respectively). These findings indicate that it is possible to create dynamically consistent full-body simulations of orthosis-assisted walking using forearm crutches if the optimal control problem is formulated appropriately.

Convergence was always better when joint rather than marker coordinates were tracked. It is not surprising that tracking markers is more difficult in terms of convergence [31]. In both cases (tracking marker coordinates and tracking joint coordinates), the optimal control solver treats joint angles as design variables. During the optimisation solution process, the optimiser adjusts the joint angle design variables so as to minimise the cost function and fulfil the constraints. When a joint angle design variable is adjusted to perform gradient calculations, it affects only that one joint angle, whereas it affects all marker positions. Furthermore, the marker positions most affected are the ones farthest from the adjusted joint angle in the same kinematic chain, creating an unequal effect on different marker positions. Thus, adjusting joint angles to minimise errors in joint angle trajectories is a straightforward uncoupled linear solution process, while adjusting joint angles to minimise errors in marker position trajectories is a more complicated coupled nonlinear solution process.

While it is true that tracking joint coordinates is easier, we also wanted to check whether accurate tracking of joint coordinates would result in accurate tracking of marker coordinates. If not, then we could consider tracking marker coordinates

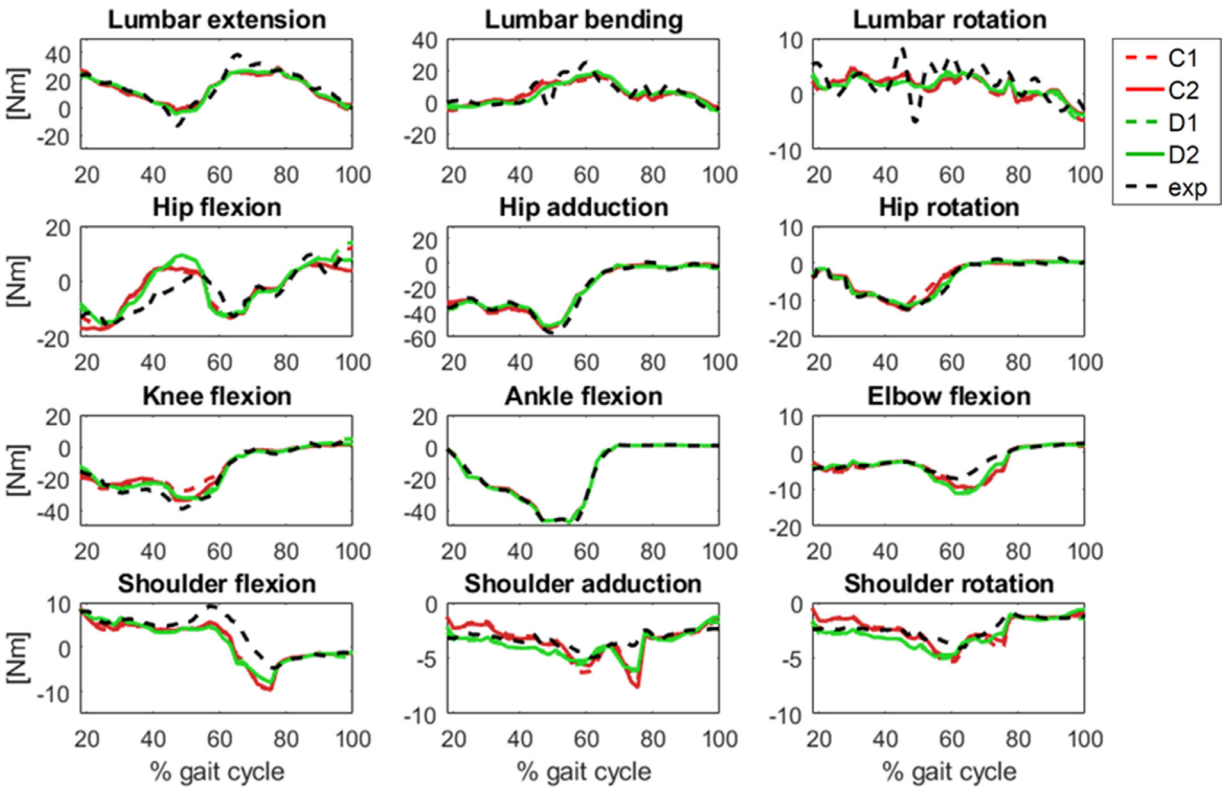

Fig. 5. Joint torques obtained in formulations C and D for the full residual reduction compared to experimental values. Results for each one of the five initial guesses are plotted for each formulation. Note that all five initial guesses converge to the same solution, as no difference is appreciated between curves from the same formulation. Results are shown for torso, right leg and right arm.

despite its higher computational cost. For this purpose, we computed RMSE for coordinates that were not being tracked for each formulation (Table 3). In formulations with ground reaction adjustments, mean RMSEs for marker coordinates were similar when tracking marker coordinates or joint coordinates. Comparing for the same residual reduction tolerance and for the same case (1 or 2), the largest error between marker coordinate mean RMSE when tracking marker coordinates and joint coordinates was 0.19 cm. In contrast, mean RMSE for angular joint coordinates was larger when tracking marker coordinates. In this case, comparing for the same residual reduction tolerance and for the same case (1 or 2), the largest error between angular joint coordinate mean RMSE when tracking marker coordinates and joint coordinates was 2.19°. These results suggest that close tracking of joint coordinates results in close tracking of marker coordinates, but not necessarily vice versa. Furthermore, since tracking joint coordinates requires fewer iterations and takes less computation time, it is preferable to track joint coordinates obtained from an IK analysis performed using experimental marker trajectories.

Our results also suggest that ground reactions should be added as controls to the optimal control problem to reduce tracking errors and minimise residuals. Marker and joint coordinate tracking are both more accurate when ground reactions are adjusted (i.e., mean RMSE is lower in formulations C and D compared to formulations A and B), and problem formulations requiring full residual reduction converge only when ground reactions are added as controls. Formulations A and B without ground reaction adjustment reached the maximum number of iterations (10,000) for the first initial guess. Though those formulations were able to converge if joint coordinate bounds were increased substantially (to 3 cm and 10°), the resulting motions were visibly unrealistic (e.g., the model walked without the feet contacting the ground). This observation suggests that for full residual reduction, it is more difficult to find a solution with low joint coordinate error bounds (1 cm and 5°) when using formulations A or B. To improve performance of these formulations, one could consider using error bounds adapted to each coordinate, or calibrating lower body joint positions/orientations in the body segments to match the subject's movement data better [38]. In contrast, if both motion and ground reactions are adjusted, then an optimal solution can be obtained within realistic coordinate error bounds. This finding suggests that including ground reactions as controls in the optimisation problem may compensate for model simplifications. In the present study, the most critical ground reactions were the crutch-ground contact forces. Since these forces were measured with respect to local crutch axes, a small error in crutch orientation could lead to large errors when transforming from the local to the global coordinate system.

Our results did not produce a clear answer to whether minimising joint accelerations or joint jerks is better. Minimisation of joint accelerations or joint jerks was needed as a regularisation term to obtain a unique solution. Based on the number of iterations, there is no clear trend between cases 1 and 2 in each formulation (Table 3). In general, minimising

accelerations (case 1) required fewer iterations and less computation time, but this difference was not significant (apart from for formulations C1 and C2 and full residual reduction). Regardless of the regularisation term used, the optimal motion and ground reactions produced by both cost functions were very similar, and there was not a clear correlation between error magnitudes and minimising joint accelerations or jerks. Marker and joint coordinate errors were lower in general when minimising joint jerk, but joint torque and ground reaction errors were lower in some formulations when minimising joint accelerations, and in others when minimising joint jerks. Therefore, we can conclude that formulations that track joint coordinates and adjust ground reactions, regardless of minimising joint accelerations or joint jerks (D1 and D2, respectively), are the ones for which the best results were obtained.

Our computation time and mean RMSE for joint coordinates are consistent with results found in the literature. Our computation time varied from about a minute to more than 5 h, and for the preferred formulations D with full residual reduction, it was less than 5 min. In Lin et al. [39], 3 to 5 h were required to track experimental data for a complete gait cycle using a 3D model with 25 DOFs and 80 muscle-tendon units (MTUs). In Meyer et al. [17], roughly 30 min were required for a torque-driven prediction using a 3D model with 37 DOFs. In Shourijeh et al. [40], 45 min were needed to obtain muscle forces tracking experimental data using a 3D model with 16 DOFs and 46 muscles. Finally, in Falisse et al. [41], about 20 min were required for tracking simulations of walking with a muscle-driven model with 29 DOFs, 92 muscles, and 12 contact spheres (6 per foot). The same model was used for predictive simulations of walking, reporting an average of 36 min of computational time [24]. These published studies included muscles in their models or predicted a new motion instead of tracking experimental data, so it is not surprising that some of them required more time than in our study. Furthermore, the obtained joint coordinate tracking results are consistent with errors reported in some of the previous studies. For formulations D with full residual reduction, the obtained mean RMSE for joint coordinates were 0.54 cm (both D1 and D2) and 0.85° (D1) and 0.77° (D2). For same errors, Lin et al. [42] reported 0.5 cm and 1.2°, while Lin et al. [39] reported 0.3 cm and 2°, which are both the same order of magnitude as the computed errors.

This study possesses several limitations related to the subject and device models and the experimental data collection. Although a real active orthosis was simulated, the model was simplified by attaching the device directly to each corresponding lower limb (modifying the mass and inertial properties of the affected segments accordingly) and assuming perfect alignment of orthosis joints and skeletal joints. We used this simplification because we were focusing on exploring optimal control problem formulation issues related to generation of dynamically consistent assisted walking motions regardless of the physical human-device interaction. Moreover, there may be errors in the orthosis mechanical properties, as the orthosis plastic parts (Fig. 1, left) were not included in the CAD model. Future work will explore modelling orthosis-body contact interactions, and will try to minimise errors in the orthosis mechanical properties through experiments. Additionally, since walking was performed with crutch assistance, a more detailed model would be recommended for the shoulder joint complex. For this situation, motion at this joint might not be well represented by a shoulder modelled as a spherical joint. During crutch walking, there is also more head motion relative to the trunk than during normal walking, so the addition of neck motion to the model could be beneficial. Finally, we did not calibrate the positions and orientations of joint axes in our skeletal model, which may have affected the accuracy of our inverse dynamics joint moments [43]. Regarding the experimental setting, the motion analysis laboratory was equipped with only two force plates, and consequently, we could not simulate a complete gait cycle. We simulated the approximately 82% of the gait cycle for which experimental data were available, instead of extrapolating the data for the other part of the cycle. In addition, for the IK analysis, we used equal weights for all markers, which may have increased the size of kinematic errors needed to achieve a dynamically consistent walking motion. Finally, not including muscle dynamics may lead to physiologically unfeasible joint torque results. Although RMSEs for formulations with ground reaction adjustments (C and D) are reasonable (around 2 Nm), we do think that adding a joint torque tracking term in the cost function may reduce those errors, and would avoid having unrealistic joint torque rates.

In conclusion, this study found that using an optimal control problem formulation that tracks joint coordinates (e.g., as obtained from an IK analysis) and experimental ground reaction forces and moments while minimising joint acceleration or joint jerk can produce efficient dynamically consistent full-body crutch walking simulations. While all formulations that converged produced dynamically consistent simulations (to the imposed level of tolerance for residual reduction), the selected exhibited the best performance overall in terms of convergence (number of iterations, computation time) and tracking errors (markers and joint coordinates, joint torques, and ground reactions). The study also contributed to identify some challenges involved in adding crutches to a walking model and applying measured crutch-ground reaction forces to the model. These findings do not depend on whether the subject is healthy or impaired, and the methodology should be equally applicable to patients with SCI (which is our long-term target). In the future, when we seek to generate novel predictive walking simulations for different active knee controller designs, we anticipate that the same approach of tracking experimental ground reactions will work well for generating an initial dynamically consistent walking motion that closely reproduces the available experimental data. Before that, we will calibrate subject-specific deformable contact models that will generate ground reaction forces and moments in predictive simulations. Therefore, a difference in the OCP formulation will be that ground reaction forces and moments currently defined as controls, which can be viewed as “ideal” contact models, will be replaced with the abovementioned compliant models. Regarding human-orthosis co-actuation strategy, in our predictive simulations we will assume that the knee active torque is fully exerted by the orthosis actuator, since the device is intended for motor complete spinal cord injured subject, i.e., with no motor function at knee muscles.

Declaration of competing interest

The authors declare that they have no known competing financial interests or personal relationships that could have appeared to influence the work reported in this paper.

Acknowledgements

We thank Marleny Arones for the introduction to the patient-specific pipeline developed at the Rice Computational Neuromechanics Lab. We also thank Nicholas A. Bianco for the discussion and his advice during the OpenSim Advanced User Workshop in March 2018 at Stanford University, which was supported by the National Institutes of Health Grant P2C HD065690 through an Outstanding Researcher Award. Also the support of the Spanish Ministry of Economy and Competitiveness (MINECO) along with the European Regional Development Fund (ERDF) under project DPI2015-65959-C3-2-R is greatly acknowledged.

References

[1] World Health Organization+++WHO Global Disability Action Plan 2014-2021: Better Health for All People with Disability, 2015.
[2] A.J. del-Ama, A.D. Koutsou, J.C. Moreno, A. De-los-Reyes, N. Gil-Agudo, J.L. Pons, Review of hybrid exoskeletons to restore gait following spinal cord injury, J. Rehabil. Res. Dev. 49 (2012) 497–514 https://doi.org/10.1682/JRRD.2011.03.0043.
[3] J.M. Font-Llagunes, D. Clos, U. Lugrís, F. Javier Alonso, J. Cuadrado, Design and experimental evaluation of a low-cost robotic orthosis for gait assistance in subjects with spinal cord injury, in: J. González-Vargas, J. Ibáñez, J. Contreras-Vidal, H. van der Kooij, J. Pons (Eds.), Wearable Robot. Challenges Trends. Biosyst. Biorobotics, Springer, Cham, 2017, pp. 281–285. https://doi.org/10.1007/978-3-319-46532-6_46.
[4] D. García-Vallejo, J.M. Font-Llagunes, W. Schiehlen, Dynamical analysis and design of active orthoses for spinal cord injured subjects by aesthetic and energetic optimization, Nonlinear Dyn. 84 (2016) 559–581 https://doi.org/10.1007/s11071-015-2507-1.
[5] K. Mombaur, Optimal control for applications in medical and rehabilitation technology: challenges and solutions, in: J.-B. Hiriart-Urruty, A. Korytowski, H. Maurer, M. Szymkat (Eds.), Adv. Math. Model. Optim. Optim. Control, 2016, pp. 103–145. https://doi.org/10.1007/978-3-319-30785-5_5.
[6] C.F. Ong, J.L. Hicks, S.L. Delp, Simulation-based design for wearable robotic systems: an optimization framework for enhancing a standing long jump, IEEE Trans. Biomed. Eng. 63 (2016) 894–903 https://doi.org/10.1109/TBME.2015.2463077.
[7] T.K. Uchida, A. Seth, S. Pouya, C.L. Dembia, J.L. Hicks, S.L. Delp, Simulating ideal assistive devices to reduce the metabolic cost of running, PLoS ONE 11 (19) (2016) https://doi.org/10.1371/journal.pone.0163417.
[8] M. Millard, M. Sreenivasa, K. Mombaur, Predicting the motions and forces of wearable robotic systems using optimal control, Front. Robot. AI. 4 (12) (2017).
[9] G. Liu, Y. Zhang, S.-Q.Q. Xie, A. Xue, Optimal control and biomechanics of ambulation with spring-loaded crutches, Int. J. Adv. Robot. Syst. 8 (2011) 1–11 https://doi.org/10.5772/10664.
[10] M. Ackermann, B.A. Taissun, A computational study of the swing phase of the gait with standard and spring-loaded crutches, in: Proc. IEEE RAS EMBS Int. Conf. Biomed. Robot. Biomechatronics, 2012, pp. 1476–1481. https://doi.org/10.1109/BioRob.2012.6290718.
[11] S. Tashman, F.E. Zajac, I. Perkash, Modeling and simulation of paraplegic ambulation in a reciprocating gait orthosis, J. Biomech. Eng. 117 (1995) 300–308 https://doi.org/10.1115/1.2794185.
[12] G. Serrancoli, A. Falisse, C. Dembia, J. Vantilt, K. Tanghe, D. Lefeber, I. Jonkers, J. De Schutter, F. De Groote, Subject-exoskeleton contact model calibration leads to accurate interaction force predictions, IEEE Trans. Neural Syst. Rehabil. Eng. 27 (2019) 1597–1605 https://doi.org/10.1109/tnsre.2019.2924536.
[13] B.N. Fournier, E.D. Lemaire, A.J.J. Smith, M. Doumit, Modeling and simulation of a lower extremity powered exoskeleton, IEEE Trans. Neural Syst. Rehabil. Eng. 26 (2018) 1596–1603 https://doi.org/10.1109/TNSRE.2018.2854605.
[14] F. Mouzo, U. Lugris, R. Pamies-Vila, J. Cuadrado, U. Lugrís, R. Pamies-Vila, J. Cuadrado, Skeletal-level control-based forward dynamic analysis of acquired healthy and assisted gait motion, Multibody Syst. Dyn. 44 (29) (2018) https://doi.org/10.1007/s11044-018-09634-4.
[15] M. Ackermann, A.J. van den Bogert, Optimality principles for model-based prediction of human gait, J. Biomech. 43 (2010) 1055–1060 https://doi.org/10.1016/j.jbiomech.2009.12.012.
[16] D. García-Vallejo, W. Schiehlen, 3D-Simulation of human walking by parameter optimization, Arch. Appl. Mech. 82 (2012) 533–556 https://doi.org/10.1007/s00419-011-0571-7.
[17] A.J. Meyer, I. Eskinazi, J.N. Jackson, A.V. Rao, C. Patten, B.J. Fregly, Muscle synergies facilitate computational prediction of subject-specific walking motions, Front. Bioeng. Biotechnol. 4 (2016) 77 https://doi.org/10.3389/fbioe.2016.00077.
[18] M.L. Felis, K. Mombaur, Modeling and optimization of human walking, in: K. Mombaur, K. Berns (Eds.), Model. Simul. Optim., 2013, pp. 31–42. https://doi.org/10.1007/978-3-642-36368-9_3.
[19] M.L. Handford, M. Srinivasan, Robotic lower limb prosthesis design through simultaneous computer optimizations of human and prosthesis costs, Sci. Rep. 6 (7) (2016).
[20] M. Sreenivasa, M. Millard, M.L. Felis, K. Mombaur, S.I. Wolf, Optimal control based stiffness identification of an ankle-foot orthosis using a predictive walking model, Front. Comput. Neurosci. 11 (13) (2017).
[21] F. De Groote, A.L. Kinney, A.V. Rao, B.J. Fregly, Evaluation of direct collocation optimal control problem formulations for solving the muscle redundancy problem, Ann. Biomed. Eng. 44 (2016) 2922–2936 https://doi.org/10.1007/s10439-016-1591-9.
[22] A.J. Van Den Bogert, D. Blana, D. Heinrich, Implicit methods for efficient musculoskeletal simulation and optimal control, Procedia IUTAM 2 (2011) 297–316 https://doi.org/10.1016/j.piutam.2011.04.027.
[23] A.D. Koelewijn, E. Dorschky, A.J. van den Bogert, A metabolic energy expenditure model with a continuous first derivative and its application to predictive simulations of gait, Comput. Methods Biomech. Biomed. Eng. 21 (2018) 521–531 https://doi.org/10.1080/10255842.2018.1490954.
[24] A. Falisse, G. Serrancolí, C.L. Dembia, J. Gillis, I. Jonkers, F. De Groote, Rapid predictive simulations with complex musculoskeletal models suggest that diverse healthy and pathological human gaits can emerge from similar control strategies, J. R. Soc. Interface 16 (2019) 20190402 https://doi.org/10.1098/rsif.2019.0402.
[25] J.M. Font-Llagunes, U. Lugrís, D. Clos, F.J. Alonso, J. Cuadrado, Design, control and pilot study of a lightweight and modular robotic exoskeleton for walking assistance after spinal cord injury, J. Mech. Robot. 12 (2020) 031008 (8 pp.).
[26] B. Chen, B. Zi, Z. Wang, L. Qin, W.H. Liao, Knee exoskeletons for gait rehabilitation and human performance augmentation: a state-of-the-art, Mech. Mach. Theory 134 (2019) 499–511 https://doi.org/10.1016/j.mechmachtheory.2019.01.016.
[27] S. Delp, F.C. Anderson, A.S. Arnold, P. Loan, A. Habib, C.T. John, E. Guendelman, D.G. Thelen, OpenSim: open-source software to create and analyze dynamic simulations of movement, IEEE Trans. Biomed. Eng. 54 (2007) 1940–1950 https://doi.org/10.1109/TBME.2007.901024.
[28] A. Seth, J.L. Hicks, T.K. Uchida, A. Habib, C.L. Dembia, J.J. Dunne, C.F. Ong, M.S. DeMers, A. Rajagopal, M. Millard, S.R. Hamner, E.M. Arnold, J.R. Yong, S.K. Lakshmikanth, M.A. Sherman, J.P. Ku, S.L. Delp, OpenSim: Simulating musculoskeletal dynamics and neuromuscular control to study human and animal movement, PLoS Comput. Biol. (2018) 14 https://doi.org/10.1371/journal.pcbi.1006223.
[29] E. Sardini, M. Serpelloni, M. Lancini, Wireless instrumented crutches for force and movement measurements for gait monitoring, IEEE Trans. Instrum. Meas. 64 (2015) 3369–3379 https://doi.org/10.1109/TIM.2015.2465751.

[30] S.R. Hamner, A. Seth, S. Delp, Muscle contributions to propulsion and support during running, J. Biomech. 43 (2010) 2709–2716 https://doi.org/10.1016/j.jbiomech.2010.06.025.
[31] N.R. Sauder, A.J. Meyer, J.L. Allen, L.H. Ting, T.M. Kesar, B.J. Fregly, Computational design of FastFES treatment to improve propulsive force symmetry during post-stroke gait: a feasibility study, Front. Neurorobot. 13 (2019) 80 https://doi.org/10.3389/fnbot.2019.00080.
[32] J.T. Betts, Practical Methods for Optimal Control and Estimation Using Nonlinear Programming, 2010 https://doi.org/10.1137/1.9780898718577.
[33] A.V. Rao, D.a. Benson, C. Darby, M. Patterson, C. Francolin, I. Sanders, G.T. Huntington, GPOPS– II: a MATLAB software for solving multiple-phase optimal control problems using hp–adaptive gaussian quadrature collocation methods and sparse nonlinear programming, ACM Trans. Math. Softw. 37 (2014) 1–39 https://doi.org/10.1145/1731022.1731032.
[34] M.W. Koch, M. Ringkamp, S. Leyendecker, Discrete mechanics and optimal control of walking gaits, J. Comput. Nonlinear Dyn. 12 (2016) 021006 https://doi.org/10.1115/1.4035213.
[35] Y. Xiang, J. Arora, K. Abdel-Malek, Optimization-based prediction of asymmetric human gait, J. Biomech. 44 (2011) 683–693 https://doi.org/10.1016/j.jbiomech.2010.10.045.
[36] J.L. Hicks, T.K. Uchida, A. Seth, A. Rajagopal, S. Delp, Is my model good enough? Best practices for verification and validation of musculoskeletal models and simulations of human movement, J. Biomech. Eng. 137 (2015) 020905 https://doi.org/10.1115/1.4029304.
[37] A. Wächter, L.T. Biegler, On the implementation of an interior-point filter line-search algorithm for large-scale nonlinear programming, Math. Program. 106 (2006) 25–57 https://doi.org/10.1007/s10107-004-0559-y.
[38] J.A. Reinbolt, J.F. Schutte, B.J. Fregly, K.H. Mitchell, B. Il Koh, R.T. Haftka, D. Alan, Determination of patient – specific multi – joint kinematic models through two – level optimization, (2005).
[39] Y.-C.C. Lin, J.P. Walter, M.G. Pandy, Predictive simulations of neuromuscular coordination and joint-contact loading in human gait, Ann. Biomed. Eng. 46 (12) (2018) https://doi.org/10.1007/s10439-018-2045-3.
[40] M.S. Shourijeh, K.B. Smale, B.M. Potvin, D.L. Benoit, A forward-muscular inverse-skeletal dynamics framework for human musculoskeletal simulations, J. Biomech. 49 (2016) 1718–1723 https://doi.org/10.1016/j.jbiomech.2016.04.007.
[41] A. Falisse, G. Serrancolí, C.L. Dembia, J. Gillis, F. De Groote, Algorithmic differentiation improves the computational efficiency of OpenSim-based trajectory optimization of human movement, PLoS ONE 14 (2019) e0217730 https://doi.org/10.1371/journal.pone.0217730.
[42] Y.-C. Lin, M.G. Pandy, Three-dimensional data-tracking dynamic optimization simulations of human locomotion generated by direct collocation, J. Biomech. 59 (8) (2017).
[43] J.A. Reinbolt, R.T. Haftka, T.L. Chmielewski, B.J. Fregly, Are patient-specific joint and inertial parameters necessary for accurate inverse dynamics analyses of gait? IEEE Trans. Biomed. Eng. 54 (2007) 782–793 https://doi.org/10.1109/TBME.2006.889187.